


Mixing in High-Pressure Polymerization Reactors: A Combined Experimental and Modeling Approach

Laura Standecke, Lena Gockel, and Markus Busch*

DOI: 10.1002/cite.202200218

 This is an open access article under the terms of the Creative Commons Attribution-NonCommercial-NoDerivs License, which permits use and distribution in any medium, provided the original work is properly cited, the use is non-commercial and no modifications or adaptations are made.

Mixing in low-density polyethylene (LDPE) reactors is crucial regarding process safety as well as process efficiency. The extreme process conditions of pressures up to 3000 bar make it difficult to get an insight into LDPE reactors. This problem is tackled by a combined experimental and modeling approach. A poly(methylmethacrylate) duplicate of a laboratory high-pressure reactor is set up to measure residence times and visualize flow lines. Experimental results are then compared to a computational fluid dynamics model.

Keywords: CFD modeling, High-pressure polymerization, Low-density polyethylene, Mixing behavior, Residence time distribution

Received: December 06, 2022; *revised:* January 19, 2023; *accepted:* February 20, 2023

1 Introduction

Polymers are a widespread product and present in our everyday lives as packaging, piping, or wire insulation. About 17.4% of the European total polymer demand falls on low-density polyethylene (LDPE) and linear low-density polyethylene (LLDPE) [1]. LDPE is produced by free-radical polymerization in tubular or autoclave reactors at temperatures up to 300 °C and pressures up to 3000 bar. The polymerization is started by a thermal initiator like an organic peroxide. By stepwise adding monomer to the resulting peroxide radical, a polymer is built. The polymerization can terminate by a reaction between two radical species. Transfer reactions lead to the characteristic long- and short-chain branches of LDPE. [2]

Knowledge on mixing in LDPE reactors is crucial of multiple reasons. At the operating pressure of a LDPE plant, the decomposition limit of ethylene is around 300 °C. Above that temperature ethylene exothermically decomposes into solid carbon, methane, and hydrogen [3]. Therefore, the formation of hot spots due to inefficient mixing is a major safety risk. In tubular reactors, imperfect mixing in radial direction leads to a formation of a polymer-rich boundary layer, the so-called fouling layer. Fouling layers reduce the heat transfer from the reactor to the cooling water and hence the conversion in the reactor. Fouling can also be responsible for a high-molecular weight shoulder in the products' molecular weight distribution that can influence the processability of the polymer. Another important topic is the efficient feed mixing especially of the peroxide initiator. Peroxide initiators have an optimum in the initiator consumption (mg initiator per kg LDPE) depending on

the polymerization temperature. Above that minimum, the initiator efficiency is reduced by an increase in chain termination due to imperfect mixing. [4]

The extreme reaction conditions of the LDPE process and the associated heavy reactor walls make it difficult to gain insight into the process. A cross-section of a high-pressure laboratory reactor is shown in Fig. 1a and illustrates the relation between reactor wall and reaction chamber. To overcome that issue and evaluate the mixing behavior of high-pressure polymerization reactors, two complementary approaches are followed. A poly(methylmethacrylate) (PMMA) duplicate of the high-pressure reactor is constructed to carry out tracer experiments. The experimental setup allows a quantitative analysis of the residence time distribution of the reactor as well as a visualization of flow lines with blue ink. In parallel a CFD (computational fluid dynamics) model is set up and validated with the experimental setup. Fig. 1 depicts the polymerization reactor as well as the PMMA reactor and the geometry of the CFD simulation.

The determination of residence time distributions is a common analysis method in chemical engineering [5] and with increasing computer power became also subject of simulation studies [5–16]. Li et al. present different methods to access the residence time via CFD simulations including

*Laura Standecke[‡], ¹Lena Gockel[‡], ¹Prof. Dr. Markus Busch (markus.busch@pre.tu-darmstadt.de)

¹TU Darmstadt, Ernst-Berl-Institut, Alarich-Weiss-Strae 8, 64287 Darmstadt, Germany.

[‡] These authors contributed equally.

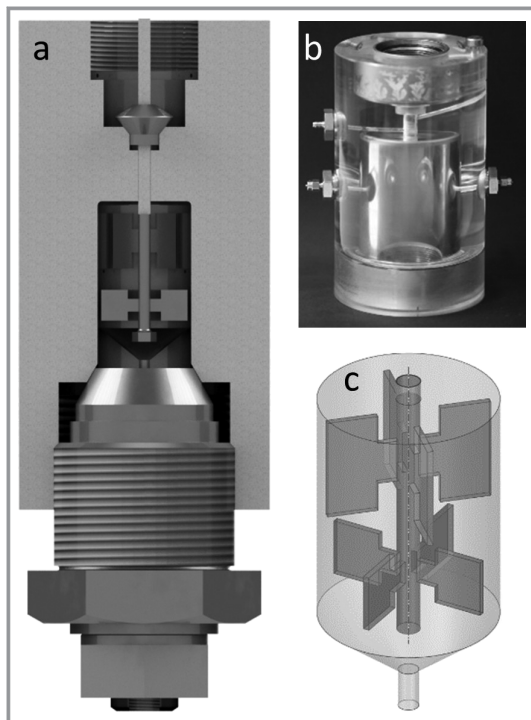


Figure 1. High-pressure laboratory reactor for polymerization experiments (a), PMMA reaction for tracer experiments (b) and geometry for CFD simulations (c). The feed is a small ring gap around the stirrer shaft.

Lagrangian particle tracking as well as solving a transport equation for a tracer species or the average residence time [6]. A comparison between experimental and simulated residence time distributions for stirred vessels can be found in literature for different applications as single-phase vessels [7, 8], gas-liquid systems [9, 10] or electrochemical reactors [11]. Besides stirred vessel, the method is also applied to, e.g., membrane reactors [12], jet mixing [13] or pump-mixer units [14]. In the field of polymerization, Gamba et al. analyzed the mixing in a styrene reactor by CFD simulation as well as tracer experiments measuring the conductivity of an injected salt solution [15]. Inglès et al. applied the planar laser induced fluorescence (PLIF) technique to the geometry of a polymerization reactor using a fluorescent tracer [16]. The present work puts the topic of residence time distribution in the context of high-pressure polymerization by showing how tracer experiments at ambient conditions can give quantitative information on high-pressure reactors despite significantly different operating conditions.

2 Experimental

Residence time distribution and mixing behavior experiments are performed with a self-constructed measuring device. The setup is constructed for performing pulse experiments with water as fluid. For these measurements, a tracer is required. A substance is appropriate as a tracer if its concentration is determinable by simple measurement techniques. Thus, dyes, electrolytes or radioactive substances can be chosen for example. The tracer is further required to be chemically inert and non-adsorbable at the reactor interior walls. It should exhibit a similar density and viscosity in comparison to the reaction medium and should be non-toxic. [17, 18]

Since water is used as fluid and there is the availability of a color sensor, blue ink is used as tracer. Density and rheological properties of the ink can be assumed to be identical to these of pure water as the used ink consists of 99 % water and aqueous ingredients.

The measuring device is characterized by the flexibility in change of reactor types, reactor, and stirrer geometries and even baffles. Furthermore, a variation of volume flows up to 160 mL min^{-1} , stirring frequencies up to 3000 rpm, viscosities up to 30 mPa s and different feeding points can be realized for investigations.

The flowsheet of the experimental setup is depicted in Fig. 2. The dosing of the fluids is realized by two pumps, Ritmo R15 and Carino 09, from Fink Chem + Tec GmbH. Thereby, the discontinuous Ritmo R15 conduces the high-volume flows, whereas the continuous double piston pump Carino 09 guarantees with its maximum 10 mL min^{-1} a pulsation-free injection. For ensuring defined and reproducible injection of tracers a sample loop valve MXP 7900-000 by IDEX Health & Science is used. The reactor is a PMMA mimic of the original steel autoclave. Additionally, the steel

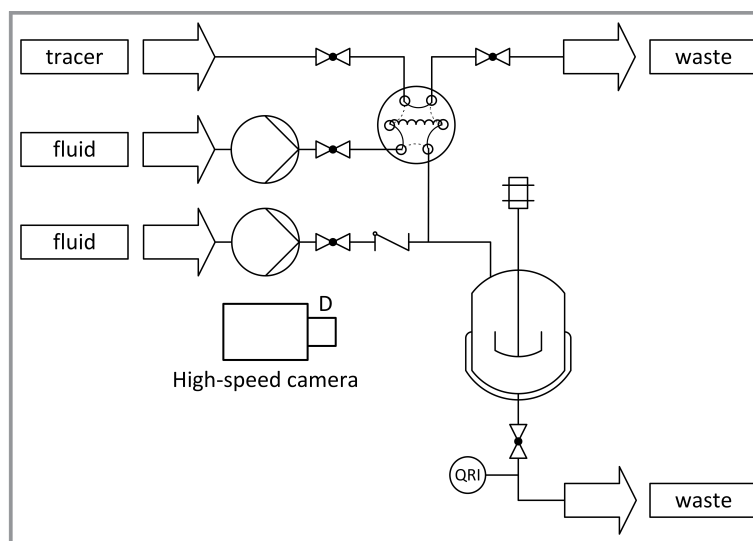


Figure 2. Flowsheet of the experimental setup. Dosing of fluids is realized by two pumps. The tracer is injected via a sample loop valve into the reactor and its concentration is measured by a color sensor directly below the reactor.

stirrer is replaced by a 3D-printed transparent version. The stirrer is powered by a Cyclone 075 from büchiglasuster, exhibiting a magnetic coupling with an electrical motor. For detecting the tracer concentration, a highly sensitive optical color sensor TCS3472 EVM by the company AMS is directly positioned below the reactor. The visual tracking of the experiments is achieved through the industrial camera uEye UI-6240RE-C-HQ R.2 by IDS Imaging Development Systems GmbH.

The introduction of a determined amount of tracer at the reactor inlet is ensured by the used sample loop valve. Here, the connection to a LabView control by National Instruments guarantees a defined pulse with a pulse time of 1 s. The objective is to obtain an input signal that can be assumed to have an infinite height in comparison to the reactor function and a width of zero. The input signal compared to the reactor function is depicted in Fig. 3.

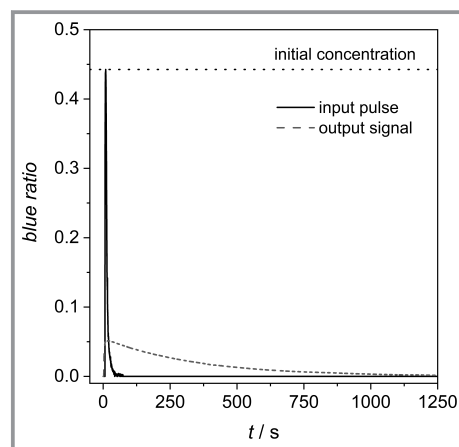


Figure 3. Comparison of input and output signal of the tracer. The input pulse is comparably narrow in contrast to the reactor function.

3 Modeling

CFD simulations are carried out with the commercial software Ansys® Fluent (Release 2021 R1). The geometry consists of a cylindrical stirred vessel as shown in Fig. 1. The stirrer rotation is modeled with a rotating reference frame. For turbulence modeling, the standard k - ε -model is used. First, a steady-state velocity field is calculated by solving the continuity and momentum equation, as well as an equation for the turbulent kinetic energy k and the turbulent dissipation rate ε . The temperature is assumed to be constant. After reaching a steady state the velocity field is frozen and a transient simulation is carried out to solve a transport equation of the tracer specie according to Eq. (1). Here ρ is the density, \mathbf{v} the velocity vector, Y the tracer mass fraction, D the mass diffusion coefficient, μ_t the turbulent viscosity and Sc_t the turbulent Schmidt number. At $t = 0$ s the tracer mass fraction at the inlet is set to one and after a pulse time of 1 s the mass fraction is set to zero. [6]

$$\frac{\partial}{\partial t}(\rho Y) + \nabla \cdot (\rho \mathbf{v} Y) = -\nabla \cdot \left[\left(\rho D + \frac{\mu_t}{Sc_t} \right) \nabla Y \right] \quad (1)$$

Thermo-physical properties of an ethylene-polymer-mixture under supercritical conditions are determined by empirical correlations [19]. The tracer is assumed to behave identical to the fluid with the same thermo-physical properties. The pure component densities of ethylene and polyethylene are given by Eq. (2) and Eq. (3) depending on temperature and pressure. With the mass-weighted mixing rule in Eq. (4) the density of an ethylene-polyethylene-mixture is calculated.

$$\rho_e = 3203.35 - 601.2 \lg(10p) - 1267.75 \lg(T) + 335.8 \lg(10p) \lg(T) \quad (2)$$

$$\rho_{pe} = (9.61 \cdot 10^{-4} + 7 \cdot 10^{-7} \cdot T - 5.2 \cdot 10^{-6} p)^{-1} \quad (3)$$

$$\rho_{\text{mix}} = \left(\frac{Y_e}{\rho_e} + \frac{Y_{pe}}{\rho_{pe}} \right)^{-1} \quad (4)$$

The empirical correlations for the viscosity of ethylene and polyethylene are shown in Eq. (5) and Eq. (6) while Eq. (7) states the mixture viscosity.

$$\eta_e = 10.25 \cdot 10^{-5} - 10.39 \cdot 10^{-6} (T - 347)^{0.3} + 4.68 \cdot 10^{-7} (10p)^{0.8} \quad (5)$$

$$\log(\eta_{pe}) = 0.227 + 2015/T + 3.33 \cdot 10^{-12} p \quad (6)$$

$$\eta_{\text{mix}} = \eta_e^{Y_e} \cdot \eta_{pe}^{Y_{pe}} \quad (7)$$

4 Results and Discussion

The combined experimental and CFD modeling approach for determining the mixing behavior inside high-pressure polymerization reactors is evaluated regarding the applicability of water as reference substance for the high-pressure polymerization. Therefore, Tab. 1 shows an overview of the operating conditions and thermo-physical properties of a polymerization experiment and the respective tracer experiment. Here, typical process conditions of a high-pressure mini-plant experiment with an operating temperature of 180 °C, a pressure of 2000 bar and a conversion of 10 % are assumed. In the tracer experiment the volumetric flow rate \dot{V} of the polymerization experiment is adopted.

Further, two CFD simulations were performed, one with water and one with the LDPE-ethylene mixture as fluid. Due to the adopted volumetric flow rate, the differences in densities and operating conditions have a neglectable impact as the residence time behavior of both simulations is nearly identical. The simulations' outcome underlines that water at room temperature is applicable as a modeling

Table 1. Comparison of operating conditions and thermo-physical properties of a tracer experiment and a polymerization experiment.

	Polymerization experiment	Tracer experiment
fluid	10 wt % LDPE in ethylene	water
p [bar]	2000	1.013
T [K]	453.15	298.15
ρ [kg m ⁻³]	526 [19]	997 [20]
η [mPa s]	0.689 [19]	0.890 [20]
\dot{V} [mL min ⁻¹]	64	64

system for the supercritical high-pressure polymerization of LDPE. This transferability has also been proven in the experimental work of Busch in 1993 [21]. In case of other polymerization systems (e.g., solution polymerization) with higher conversions and thus higher viscosities, water glycerol mixtures can be used as fluids.

The comparison is drawn between the experimental model system water and the LDPE CFD model with a polymer content of 10 wt % at 180 °C and 2000 bar. The stirring frequency is varied and the impact on the hydrodynamic behavior compared. Fig. 4 depicts the residence time distributions in dependence of time for a) 800 rpm, b) 100 rpm, and c) 0 rpm.

In general, the residence time distributions of experiment and CFD simulation are in good agreement. At a stirring frequency of 0 rpm, the maximum is in experiment and simulation explicitly higher than at 100 rpm and 800 rpm. This is caused by the presence of short-circuiting as the tracer is not mixed in after the pulse but directly shot to the reactor outlet. The maximum of the residence time distribution at 100 rpm is shifted to a higher residence time compared to 800 rpm what indicates a longer mixing time at lower stirrer frequencies. A slight increase of all maxima of the simulated curves in contrast to the experimental ones and small deviations in the curve shape, more differing with lower stirring frequencies, are identifiable. Better agreement between experiment and simulation can potentially be gained with a more complex turbulence model on cost of a higher simulation time. The Reynolds stress model would for example account for the anisotropy of the flow. When leaving the group of RANS (Reynolds-averaged Navier-Stokes) models, a large eddy simulation (LES) has the potential to resolve smaller flow structures. This would also be necessary to capture the flow lines shown in Fig. 5, especially for lower stirrer frequencies.

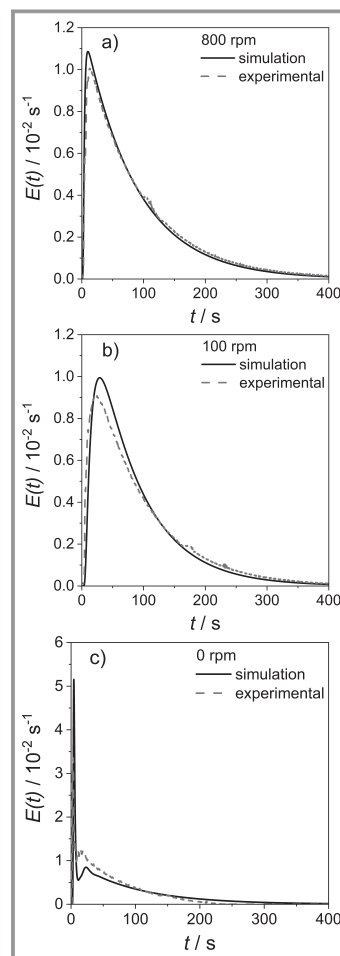


Figure 4. Comparison of the experimental and simulated residence time distributions at different stirrer frequencies.

The time-resolved pictures for all stirring frequencies show that blue ink is a suitable tracer for the flow behavior visualization. Since blue ink ensures a distinct contrast in the picture of the transparent reactor, the flow lines are made visible. Furthermore, the mixing behavior changes with the stirrer frequency. At 0 rpm, the tracer is directly flowing to the reactor outlet and the mixing takes place

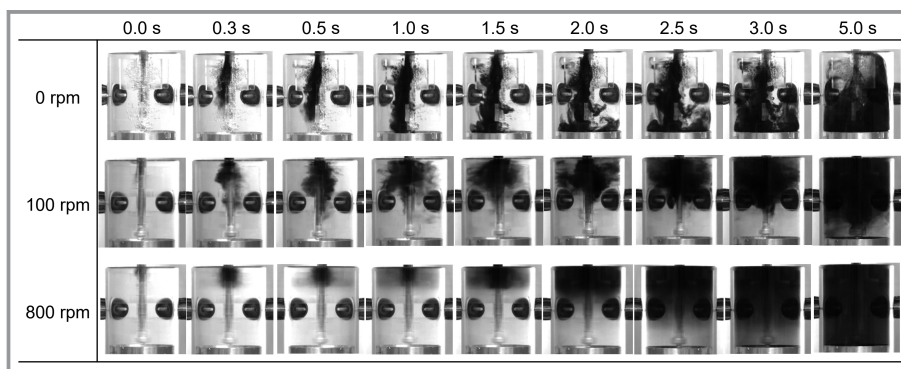


Figure 5. Experimental visualization of flow lines at different stirrer frequencies for the first period after the injection of the tracer.

from bottom to top. This short-circuiting matches with the residence time distribution results. For a stirring frequency of 100 rpm, the short-circuiting is much less pronounced and the mixing in of the tracer is rather from top to bottom. In contrast, the tracer is directly mixed in from top to bottom for 800 rpm with a mixing time of only 5 s.

5 Conclusion and Outlook

A model approach for describing the mixing behavior in high-pressure polymerizations was presented. Therefore, an experimental measuring device was set up, realizing reproducible pulse experiments with water as fluid and ink as tracer. This fluid-tracer-system proves to be a suitable model system for illustrating the mixing in LDPE reactors. Using this setup, a CFD model can be validated as the experimental residence time distributions are in good agreement with the simulation. This work exemplifies the different flow behavior inside reactors depending on the stirrer frequency.

Future efforts can now concentrate on extending the CFD model with the polymerization kinetics. Especially the mixing of the initiator feed is of major interest regarding the initiator efficiency. Furthermore, with the experimental setup and the CFD model in combination, there could be attempts to scale-up reactors and predict new stirrer geometries.

Acknowledgment

The authors gratefully acknowledge the computing time provided to them on the high-performance computer Lichtenberg at the NHR Centers NHR4CES (National High Performance Computing Center for Computational Engineering Science) at Technical University Darmstadt. This is funded by the Federal Ministry of Education and Research, and the state governments participating based on the resolutions of the GWK (Gemeinsame Wirtschaftskonferenz) for national high-performance computing at universities. Open access funding enabled and organized by Projekt DEAL.

Symbols used

D	$[m^2s^{-1}]$	mass diffusion coefficient
E	$[s^{-1}]$	residence time distributions
k	$[m^2s^{-2}]$	turbulent kinetic energy
p	[bar]	pressure
Sc_t	[-]	turbulent Schmidt number, 0.7
t	[s]	time
T	[K]	temperature
\mathbf{v}	$[m\ s^{-1}]$	overall velocity vector
\dot{V}	$[mL\ min^{-1}]$	volume flow
Y	[-]	mass fraction of tracer

Greek letters

ε	$[m^2s^{-3}]$	turbulent dissipation rate
η	$[mPa\ s]$	dynamic viscosity
μ_t	$[m^2s^{-1}]$	turbulent viscosity
ρ	$[kg\ m^{-3}]$	density

Sub- and Superscripts

e	ethylene
mix	mixture
pe	polyethylene

Abbreviations

CFD	computational fluid dynamics
LES	large eddy simulation
LDPE	low-density polyethylene
LLDPE	linear low-density polyethylene
PMMA	poly(methyl methacrylate)
RANS	Reynold-averaged Navier Stokes

References

- <https://plasticseurope.org/knowledge-hub/plastics-the-facts-2021/> (Accessed on September 05, 2022)
- G. Luft, *Chem. Unserer Zeit* **2000**, *34* (3), 190–199. DOI: [https://doi.org/10.1002/1521-3781\(200006\)34:3<190::AID-CIUZ190>3.0.CO;2-V](https://doi.org/10.1002/1521-3781(200006)34:3<190::AID-CIUZ190>3.0.CO;2-V)
- G. Luft, J. Broedermann, T. Scheele, *Chem. Eng. Technol.* **2007**, *30* (6), 695–701. DOI: <https://doi.org/10.1002/ceat.200600270>
- G. Luft, H. Bitsch, H. Seidl, *J. Macromol. Sci.* **1977**, *11* (6), 1089–1112. DOI: <https://doi.org/10.1080/0022337708061313>
- A. E. Rodrigues, *Chem. Eng. Sci.* **2021**, *230*, 116188. DOI: <https://doi.org/10.1016/j.ces.2020.116188>
- G. Li, A. Mukhopadhyay, C.-Y. Cheng, Y. Dai, in *Proc. of the ASME Fluids Eng. Div. Summer Conf.*, ASME, New York **2010**, 295–304. DOI: <https://doi.org/10.1115/FEDSM-ICNMM2010-30771>
- B. S. Choi, B. Wan, S. Philyaw, K. Dhanasekharan, T. A. Ring, *Ind. Eng. Chem. Res.* **2004**, *43* (20), 6548–6556. DOI: <https://doi.org/10.1021/ie0308240>
- A. W. Patwardhan, *Ind. Eng. Chem. Res.* **2001**, *40* (21), 5686–5695. DOI: <https://doi.org/10.1021/ie0103198>
- J. Ding, X. Wang, X.-F. Zhou, N.-Q. Ren, W.-Q. Guo, *Bioresour. Technol.* **2010**, *101* (18), 7005–7013. DOI: <https://doi.org/10.1016/j.biortech.2010.03.146>
- M. Jahoda, L. Tomášková, M. Moštík, *Chem. Eng. Res. Des.* **2009**, *87* (4), 460–467. DOI: <https://doi.org/10.1016/j.cherd.2008.12.006>
- R. Thilakavathi, D. Rajasekhar, N. Balasubramanian, C. Srinivasakannan, A. Al Shoaibi, *Int. J. Electrochem. Sci.* **2012**, *7*, 1386–1401.
- M. Brannock, Y. Wang, G. Leslie, *Water Res.* **2010**, *44* (10), 3181–3191. DOI: <https://doi.org/10.1016/j.watres.2010.02.029>
- L. Furman, Z. Stegowski, *Chem. Eng. Process.* **2011**, *50* (3), 300–304. DOI: <https://doi.org/10.1016/j.cep.2011.01.007>

- [14] K. K. Singh, S. M. Mahajani, K. T. Shenoy, S. K. Ghosh, *Ind. Eng. Chem. Res.* **2007**, *46* (7), 2180–2190. DOI: <https://doi.org/10.1021/ie061102m>
- [15] I. L. Gamba, S. M. Damian, D. A. Estenoz, N. Nigro, M. A. Storti, D. Knoeppel, *Int. J. Chem. React. Eng.* **2012**, *10* (1). DOI: <https://doi.org/10.1515/1542-6580.3057>
- [16] X. Inglès, J. Pallares, M. T. Larre, L. Méndez, F. X. Grau, *J. Ind. Eng. Chem.* **2013**, *19* (4), 1251–1256. DOI: <https://doi.org/10.1016/j.jiec.2012.12.025>
- [17] *Technische Chemie* (Eds: M. Baerns, A. Behr, A. Brehm, J. Gmehling, K. O. Hinrichsen, H. Hofmann, R. Palkovits, U. Onken, A. Renken), Wiley-VCH, Weinheim **2013**.
- [18] E. Müller-Erlwein, *Chemische Reaktionstechnik*, Springer Spektrum, Wiesbaden **2015**.
- [19] A. Buchelli, M. L. Call, A. L. Brown, *Ind. Eng. Chem. Res.* **2005**, *44* (5), 1474–1479. DOI: <https://doi.org/10.1021/ie040157q>
- [20] *VDI-Wärmeatlas*, Springer, Heidelberg **2006**.
- [21] M. Busch, *Kontinuierliche Excimerlaser-induzierte Polymerisation von Ethen in einem Hochdruck Rührkessel*, Ph.D. Thesis, Georg-August-Universität zu Göttingen **1993**.